Australasian Conference on Robotics and Automation (ACRA), December 2-4, 2009, Sydney, Australia

Characterisation of the Novint Falcon Haptic Device for Application as a Robot Manipulator

Steven Martin
Queensland University of Technology
Brisbane, Australia
steven.martin@csiro.au

Nick Hillier
CSIRO ICT Centre
Brisbane, Australia
nick.hillier@csiro.au

Abstract

The Falcon is a relatively inexpensive 3-DOF haptic device made by Novint for the gaming industry. The controller uses a form similar to that of the delta-robot configuration and because of this form, makes an interesting apparatus for research into control and estimation problems for robots involving parallel linkages. This paper presents the results of work conducted by the Autonomous Systems Lab at CSIRO in characterising the Falcon's geometric, inertial and actuation properties for application to future model-based robotic algorithm development. Some comments are made towards assessing the Falcon's suitability as an easily accessible research platform for these tasks. The aim of the paper is the presentation of the key kinematic and dynamic parameters for the device.

1 Introduction

The delta-robot configuration was introduced by Reymond Clavel in 1987 [Clavel, 1989] and provides a mechanism with three linear or rotational actuators mounted to the base, and a series of kinematic parallelograms to constrain the motion of an end-effector to translational degrees of freedom (DOF) only. This form has proven itself as an excellent platform for high-speed pick-and-place operations due to the mechanism's low actuated inertia, high power to weight ratio, high stiffness and high payload capability when compared to serial counterparts [Olsson, 2009]. In general, robotic arms that incorporate a high degree of parallelism in their design display these beneficial properties when compared to those that are primarily serial in kinematic structure. However this comes with a significant increase in the complexity of the control and both kinematic and dynamic modelling of such mechanisms.

Despite this, the delta-robot form is gaining commercial popularity as evidenced by the current influx of robots incorporating Clavel's original design (and slight variations thereof). Some examples include the 4-DOF research robot developed at the University of Western Australia [Miller, 2001], the ABB IRB 340 and the Adept Quattro s650. This configuration has also been adopted by a number of haptic devices, primarily to take advantage of the increased actuation stiffness, including Novint's Falcon, under consideration here, and Force Dimension's Omega.x and Delta.x products.

The Novint Falcon (Figure 1) uses a translational only, 3-DOF variant of the delta-robot configuration most similar to that proposed by Tsai [Tsai, 1997], whereby the spherical joints of Clavel's design are replaced by single DOF rotary joints only. The Falcon's design also incorporates a removable end-effector that can be replaced with different grips, for example a pistol-like grip designed for use in first-person shooter games, or other custom attachments such as a pen-holder or gripper. The device is already seeing application in robotics and haptics outside of the gaming industry, arguably due to its accessibility. [Schill *et al.*, 2008] presents its use as a force feedback teleoperation device whilst [Palsbo *et al.*, 2008; Streng, 2008] present a mechanical linkage and additional software that allow the Falcon to be used as a pantograph for robot-assisted repetitive motion training. It is our intention to use the Falcon as a robotic arm/manipulator rather than as an input device, and our work with the Falcon so far has proffered very little against its utilisation in this manner despite this application being contrary to its intended use. Demonstration videos of the work by Obslap Research in the *My Scrivener* product show the Falcon being used in conjunction with a pantograph as a robotic arm to write letters on paper.

The significant non-linearities in the system kinematics and dynamics of many parallel mechanisms make control and estimation tasks for this class of robots difficult using classical methods. In particular, the task of creating (planning) and executing time-minimal trajectories for robotic arms containing closed-kinematic loops

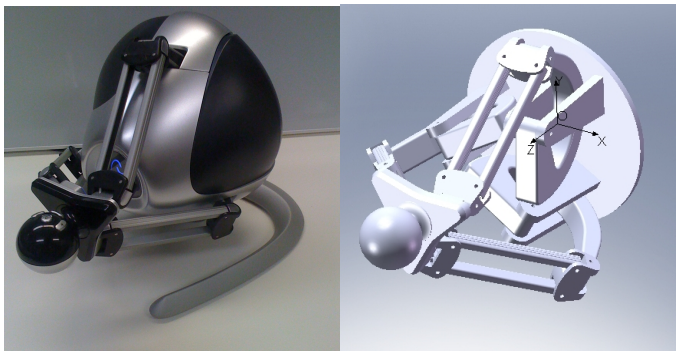

Figure 1: A photograph and CAD model generated by the authors of the Novint Falcon haptic device.

and having multiple DOFs is considered a difficult task and is an active area of research [Huang *et al.*, 2007; Pietsch *et al.*, 2003; 2005]. The delta-robot configuration, whilst a relatively simple parallel robot design, displays significant non-linear characteristics in the system kinematics and dynamics, which we consider makes it an ideal candidate for investigating and developing model based control and estimation methods for parallel robots.

This paper aims to quantify some characterising properties of the Novint Falcon, to allow the development of a dynamic model incorporating appropriate workspace constraints for subsequent use in model-based prototype trajectory generation, estimation and control methodology research for general robotic manipulators, including both those containing open and closed-kinematic forms. Whilst the manufacturer provides some basic specifications on workspace size and forces the device is able to realise, they do not describe the values in sufficient detail for modelling or control purposes.

2 Interface

The Falcon device utilises a USB interface with commands sent from the controlling computer interpreted by onboard firmware to provide actuation. Sensory data from encoders is transmitted back to the controlling computer in a similar manner. Novint has released a Windows only SDK, however for this work the open-source, cross-platform driver libnifalcon [Machulis, 2009] has been used on the linux platform.

This interface uses a 1kHz update rate with commanded forces maintained by the firmware for 100ms unless overwritten. The authors found that a 1kHz update rate was unable to be sustained over the USB interface, and typically missed commands or reads resulted in a real-world communication rate between 800Hz and 1kHz, depending on the controlling computer's load. This interface also resulted in a noticeable (2-5 samples) delay between force commands being issued and changes in the encoder measurements being received by the controlling computer. The exact cause of this delay is unknown. The simulation model developed (Section 6) updated the control loop at 800Hz and also incorporated a 2 sample communication delay at the motor interface to simulate this behaviour. It is possible that some of these delays may be eliminated with custom firmware on the Falcon's internal controller chip, but this has not been investigated by the authors.

3 Geometric and Inertial Properties

The work presented by [Grotjahn *et al.*, 2004] provides a means for system identification of the governing friction and rigid-body dynamics specifically for parallel kinematic mechanisms in a form amenable to model-based control (applied to yet another delta-robot variant). They apply a method that is a variation of the typical parameter estimation methodology of trajectory execution and least-squares (or other optimisation) parameter estimation that is commonly applied to the estimation problem for serial mechanisms. Despite the existence of this and other such methods, we have chosen to use more direct, classical measurement methods where practical in the hope that an accurate base-line could be formed. This choice was motivated in part by the often large discrepancies inherent between the estimates produced by slight variations of the estimation technique employed, see for example, the work presented by [Corke and Armstrong-H'elouvry, 1994] on forming a consensus for the parameters of the PUMA 560 serial robot arm. Similarly, such parameters as estimated by a semi-automated approach may be able to accurately model the overall behaviour of the mechanism, but do not necessarily accurately characterise discrete internal model parameters such as individual link masses.

In alignment with the direct approach, a Falcon haptic device was disassembled to allow inertial and geometric characterisation. The link masses were measured with a set of scales. Link centre-of-mass was able to be measured by freely hanging the component from a pivot and comparing the pose of the link with that of a vertical plumb-line. Repetition with multiple pivot points on the component allow the centre-of-mass to be triangulated. Similarly, the mass-moment of inertia of a component can be determined by triaxial pendulum analysis, where the period of oscillation in orthogonal planes gives rise to the inertia tensor. For most links of the Falcon, full triaxial analysis is not required due to the planar motion of the components, for example the main leg links that connect to the base can only rotate around a single pivot (and the second mass moment of inertia is sufficiently characterised by a single term in one plane), and the end effector is constrained to translational motions only. A "sanity" check was made by comparison of

dimension	value (m $\times 10^{-3}$)
a	60.0
b	102.5
c	15.7
d	11.5
e	11.5
f	26.2
g	27.9
r	36.6
s	27.2

Table 1: Key geometric properties for the links of the Novint Falcon. Labelling corresponds to that shown in Figure 3.

	leg	shin bar	shin joint	end effector
mass $\times 10^{-3}$	89.59	8.37	10.42	82.73
C.M.†				
$x \times 10^{-3}$	-3.19	56.35	15.61	15.7
$y \times 10^{-3}$	23.34	0	0	26.2
$z \times 10^{-3}$	0	0	0	48.78
I_{xx}	-	-	-	
I_{yy} $\times 10^{-6}$	-	8.5	-	-
I_{zz} $\times 10^{-6}$	140	8.5	0.7	-

Table 2: Inertial properties for the links of the Novint Falcon. Units are S.I. † Centre-of-mass, defined as a triple (x,y,z) with the x-direction along the line from parent to child joints, working outwards from the base.

the experimentally derived values to those provided by a solid modelling package.

A summary of the results of this characterisation are presented in Tables 1 and 2.

4 Motor Characterisation

The Novint Falcon is actuated by three Mabuchi RS-555PH-15280 motors whose motion can be monitored by a coaxial 4-state encoder with 320 lines per revolution. These motors are directly coupled to a 14.25 mm diameter drum, upon which a 0.5 mm diameter cable is wrapped. The cable runs around the outer edge of the main leg links at a radius of 56.0mm, and is tensioned by a spring at the inner end of the leg. This arrangement allows for a very low friction and robust actuation mechanism effectively providing a 7.62:1 (outer leg radius to drum radius, plus correction for cable width) gain to the motor output about the main leg's pivot without resorting to the use of gears.

The simple motor model presented in Equation 1 provides sufficient characterisation of the motor for our purposes, translating a commanding software torque T_c in the unit-less range -4096 to 4096, to an applied output torque T_o (N.m), in terms of a static torque gain K_s, a dynamic torque gain K_d (incorporating back-EMF and frictional effects) and the motor's rotational velocity, $\dot{\theta}$ (rad/s).

$$T_o = T_c(K_s + K_d\dot{\theta}) \tag{1}$$

It was found that values of $T_c \geq 2500$ saturated the motor input (i.e. T_o did not increase further) in static testing, although this figure changed slightly depending on the motor and unit under consideration. When the motor was in motion this limit appeared to be removed, suggesting an overload protection or similar function in the controlling firmware. The magnitude of T_c can not exceed 4096.

To determine the static motor parameter K_s, a commanding torque of T_c was applied to balance the torque of a known hanging mass via a simple PD controller. This was repeated for 6 masses (0.1 and 0.6kg) and 10 trials per mass. The effect of static friction was averaged out by initialising the control loop so that the motor was in motion, with the initial motion of the mass moving upwards in half the trials, and downwards in the remainder.

To calculate dynamic motor parameter K_d a the model for the motion of the of the motor was defined (Equation 2), incorporating the torque due to a hanging mass T_w and the combined inertial effect of the mass and motor I.

$$\ddot{\theta} = (T_o - T_w)/I \tag{2}$$

By taking the laplace transform of Equation 2 and solving for the angular displacement of the output shaft as a function of time, Equation 3 was derived.

$$\theta = A(1/Bt + 1/B^2e^{Bt}) \tag{3}$$

Where constants A and B are as per Equations 4 and 5:

$$A = (K_sT_c - T_w)/I \tag{4}$$

$$B = K_dT_c/I \tag{5}$$

K_d was estimated by fitting experimental data obtained from raising the hanging masses at given commanding force values to Equation 3 (Figure 2). This gives approximations for A and B, and hence K_d and I were solved using the value of K_s as per the results of static testing. The combined inertial magnitude I, consists of the inertial properties of the hanging weight I_w and the motor I_m. As the mass moment of inertia for the hanging weight is known, the motor's inertia can be I_m computed. Table 3 presents the identified motor parameters.

K_d	K_s	I_m
1.3779×10^{-8}	1.9835×10^{-5}	1×10^{-5}

Table 3: Motor properties for the simple motor model used in this work. The motor inertia was implemented in the simulation model by scaling by the gearing ratio squared and adding to the leg I_{zz}.

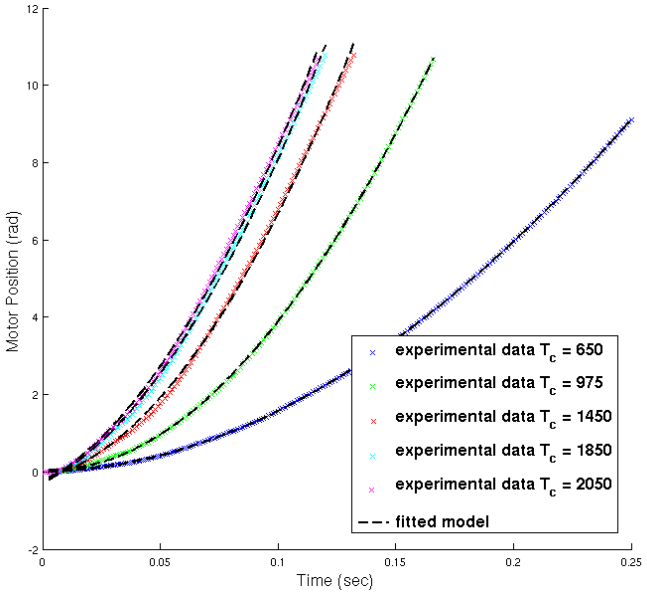

Figure 2: Plot of the dynamic motor characterisation data, showing the raw data and fitted motor model for the hanging masses of 0.1 kg and various values of T_c.

5 Kinematics

The position of the end effector is described by the triple (x, y, z) with the x-direction defined as horizontal and the z-direction perpendicular to the base. Each leg has an equal angular spacing of $2\pi/3$ around the z axis, with the top-most leg having an offset of $-\pi/12$ radians (15^0) measured from the vertical. For convenience of parameterisation, a second coordinate frame is defined in the plane of a leg (u, v, z) with u in the $x - y$ plane. In the home position (encoder values of zero), the angle from the base-leg joint to the leg-shin joint (angle of line a to the z-axis in Figure 3) is approximately 50^0.

5.1 Inverse Kinematics

The inverse kinematic problem is that of solving for required encoder values that would yield a given end-effector location. This problem is the simpler due to the redundant constraints of the mechanism. Figure 3 shows that the offset in the v direction is due only to the internal parallelogram angle θ_p. By transforming the end-effector location (x, y, z) to the frame of the arm (u, v, z) we can solve for θ_p. This then allows the application of simple 2-D Pythagorean relationships to to solve for the remaining kinematics in the $u - z$ plane analytically [Stamper, 1997].

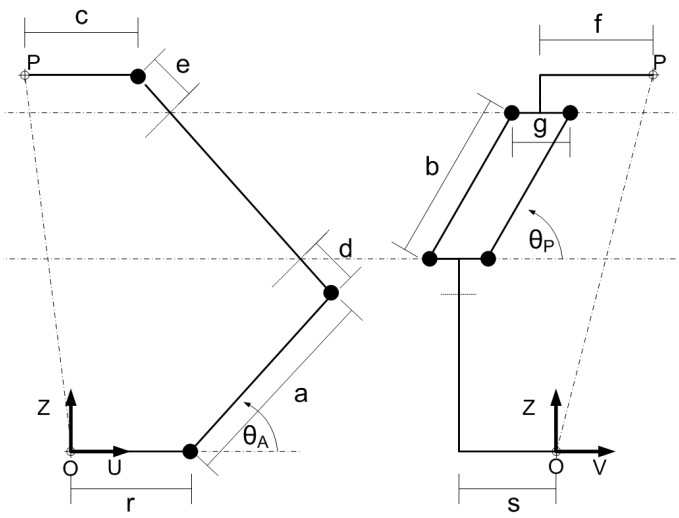

Figure 3: Labelling used to describe the geometric and kinematic properties of the Falcon. Point "P" is the end-effector location, "O" is the centre of the base as per the labelling of the CAD model in Figure 1.

5.2 Forward Kinematics

The forward kinematic problem is that of solving for the location of the end-effector, given the encoder values at the motors. This is the most useful form for the Falcon's intended use as an input device. Due to the coupled form of the delta mechanism, there admits at least 16 solutions for the end-effector position given any (viable) set of encoder values. [Stamper, 1997] presents a polynomial that provides a direct solution for the forward kinematics of a delta-robot that yields 32 solutions, of which 16 are in the real domain and correspond to those kinematically achievable if there were no joint limits. These solutions can be reduced to the single "correct" solution by simply retaining the result with the greatest value in the z direction and discarding all others.

The method preferred here and as implemented in the libnifalcon driver is that presented by [Ouellet, 2008]. The method utilises an iterative solver to compute the solution to a set of simultaneous equations produced by a series of intersecting spheres. The method is analogous to the planar case of solving the kinematics for a planar four-bar whereby a circle is described around each joint, with radius equal to the distance between this, and the connecting joint. The intersection of the circles provide the kinematically consistent solutions as a set of loop closure constraint polynomials. This governing set of equations are formed into a Jacobian transform

used to estimate the optimisation gradient for a multi-dimensional Newton-Raphson solver.

To allow for robust and correct handling of the multiple solutions without the computational load of calculating all solutions and selecting that which is correct, the iterative optimisation method can be employed in conjunction with a look-up table generated from the inverse kinematics. The look-up table provides nearby seeding values for the optimisation process. This adaptation of the standard technique is also employed in libnifalcon, although at the time of writing, the governing lookup tables use a leg offset value for the home position of 30^0 (as opposed to the authors' measured 50^0).

For the authors' work, the convergence criterion for the iterative solution process was in the encoder space. We seeded the analytical solution provided by the inverse kinematics with the end-effector location given by the current iteration of the forward kinematic solver. The corresponding encoder values were then compared against the actual and the method iterated until a convergence error of 0.5 encoder units.

5.3 Workspace

The most common criticism of the delta-robot form is the limited workspace. The three limbs of the Falcon work in kinematic (and with an appropriate control methodology, dynamic) concert to actuate the end-effector, but each leg is limited by the reach of the connected linkages. This results in a workspace bounded by warped tri-hemispherical regions overlapping along the common longitudinal (z) axis.

To quantify this volume, a number of random points were generated in Cartesian space and tested to see if they were kinematically realisable. As the number of random points were increased, so a better estimate of the workspace volume was formed. Similarly, by simple application of limit theory, we can also estimate the enclosing volume to be approximately $7.90 \times 10^{-5} m^3$. Figure 4 shows the resultant calculated plots of the workspace. The results display a symmetry about the z axis in 120^0 sectors, but also show an offset due to the non-Cartesian alignment of the actuating legs and the 15^0 rotational offset of the legs described in Section 5. The matlab data file used to generate Figure 4 has been kindly hosted by the libnifalcon wedbsite [Machulis, 2009] for access by readers.

5.4 Workspace Resolution

The theoretically minimal achievable error is defined by the minimal amount of motion that the end-effector would undergo for a single count change at the encoders, provided there was no slop or backlash in the system. This is equivalent to describing the effective theoretical resolution of the robot in the end-effector space. We can evaluate this by perturbing the motion of the actuators and solving the forward kinematics. Alternatively, (and in practice, more desirably) we can choose a minimum desired workspace resolution based on the application at hand, and solve for the maximal encoder error to achieve this resolution. This aids in motor/encoder-space controller specification and also allows for a more tolerant bound on the convergence of the kinematic solver.

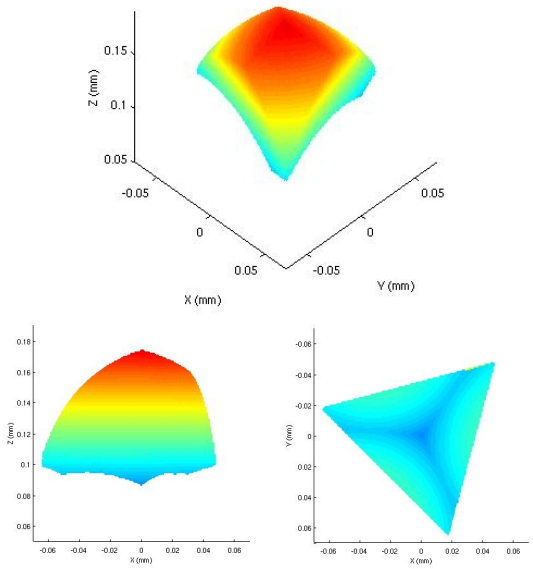

Figure 4: Plot of the Falcon's achievable workspace, points are coloured by distance along the z-axis. An isometric view (top), from the side (X-Z plane bottom-left) and from behind (X-Y plane bottom-right). Units are meters.

Figure 5 presents a plot of the 1mm end-effector error in Cartesian-space for the Falcon mapped to the encoders as described above. This plot was generated by randomly sampling the workspace in a manner similar to that presented in Section 5.3 and then choosing 6 neighbours offset by 1mm in each of the principal coordinate directions. For each point, the corresponding change in encoder values was computed and then averaged to provide a statistic describing the 1mm end-effector resolution.

As expected, the highly non-linear nature of the kinematics is revealed, with end-effector locations that are nearer to the centre of the workspace displaying higher sensor resolution, with the lowest end-effector error achievable when all three legs are at the midpoint of their stroke. The average over the entire workspace is 30 encoder counts per 1mm positioning error.

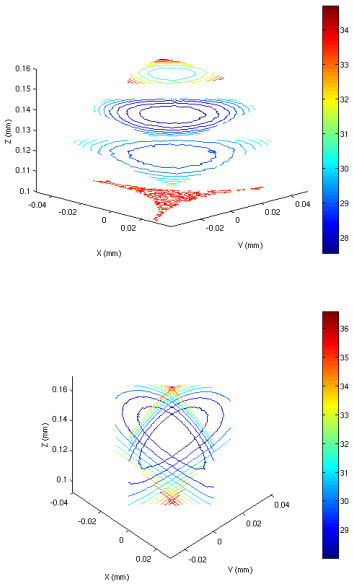

Figure 5: Plot of the 1mm end-effector error space for the Falcon mapped to the encoders. Axis units are meters, colours are mapped to encoder counts.

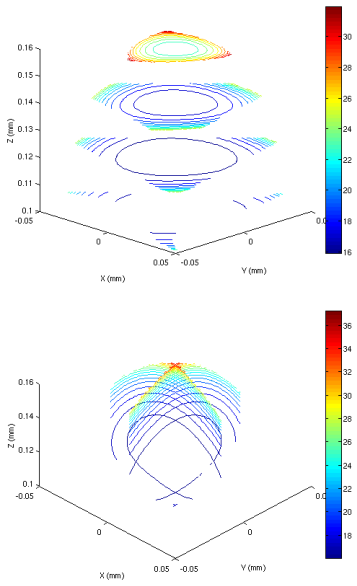

Figure 6: Plot of required torque about the leg pivot to produce 3N of force at the end-effector in the Z direction. Axis units are meters, colours are mapped to required torques (N.m).

5.5 Cartesian Force Mapping

The Jacobian derived for the solution of the forward kinematics provides a simple transform for motor torques to end effector torques (as utilised by [Stamper, 1997]). Using the Jacobian, the motor torques can be found from the end effector forces, the inverse Jacobian gives the opposite transform. Figures 6, 7 and 8 shows the root-mean-squared torque applied about the leg pivots, required to produce a force of 3N in the z,x and y directions. This analysis shows that the torques required to produce this force increase as the actuators near the end of their stroke, with the largest forces able to be generated in the centre of the workspace.

The required commanding forces to produce output forces in the X and Y direction show the dependence on actuator orientation in the workspace. The most efficient force mappings occur near the planes of the actuator legs aligned most closely to the direction of the force. This is most easily discernible in the Y direction, in which the upper actuator is only offset by 15^0 from the direction of applied force, resulting in a bias in the force mapping to the left-hand side of the device.

6 Validation

The above work has provided estimates of the key parameters required to characterise a dynamic model of the Falcon device. Such a model was subsequently implemented into the SimMechanics dynamic modelling environment [Wood and Kenedy, 2003]. To test the model, a simple proportional-derivative controller (P gain 10, D gain -0.1) operating in the robot's motor/encoder-space was implemented and a simple point-to-point step input trajectory executed in both simulation and on the Falcon. Comparison was then made of the actual executed trajectory in the motor/encoder-space and of the motor commands sent by the controllers to execute the trajectory. This simple experiment tests the parameter estimates for both static and dynamic motions. Figure 9 presents the results of this testing.

Those parameters that significantly affect the static motion of the device (masses, geometry, proportional controller gain and the motor parameter K_s) can be confirmed by comparison of the steady-state values for the encoder and controller forces, both before and after the step input. Here it can be seen that there is good correspondence, with an error in the steady state encoder value ranging from 1 to 36 encoder counts (up to 1.2^0 error at the base-leg joint), and commanding force value, from 0.2% to 8.6% of full-scale range over four experimental trials. The variation is most likely attributable to (unmodelled) static friction, indeed it was found that "bumping" the Falcon end effector would result in a slightly different experiment settling value.

Those parameters that significantly affect the dynamic motion of the device (and were not confirmed by the static experiment: inertias, differential controller gain and the motor parameter K_d) can be confirmed by com-

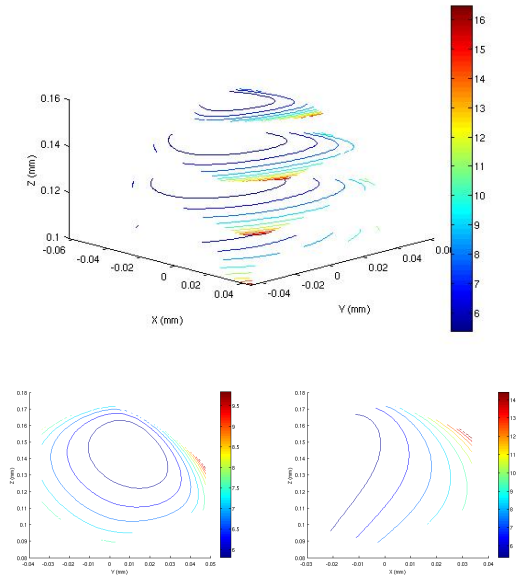

Figure 7: Plot of required torque about the leg pivot to produce 3N of force at the end-effector in the X direction. Axis units are meters, colours are mapped to required torques (N.m).

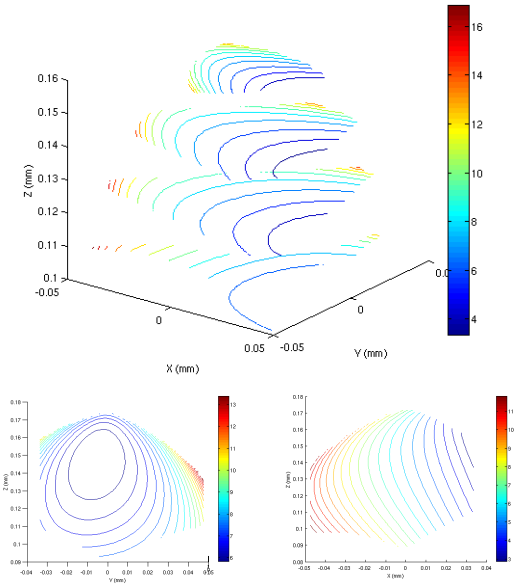

Figure 8: Plot of required torque about the leg pivot to produce 3N of force at the end-effector in the Y direction. Axis units are meters, colours are mapped to required torques (N.m).

parison of the transient for the encoder and controller forces during the execution of the trajectory. The results show that there is a good correspondence between the model in simulation and the real Falcon. The most notable error is the extra damping inherent in the data obtained experimentally that is not present in the model. The simulation relies on the differential term in the controller and the dynamic motor parameter K_d to dissipate energy from the system; friction in the joints is unmodelled. It is believed that the lack of joint friction is the primary cause of this error.

Minimal attempts have been undertaken by the authors to evaluate the static and dynamic joint friction for this device due to the lack of a simple direct measurement method for such a task. The Falcon has three degrees of freedom, however for all but the base-leg joint, these degrees of freedom result in a system that is inexorably coupled, rendering traditional friction estimation techniques as commonly performed on serial robotic arms inapplicable to the Falcon. Friction estimation methods are available that would be applicable to this device (e.g. [Grotjahn *et al.*, 2004]), but have not been applied here.

7 Conclusion

The work presented here has characterised the Novint's Falcon haptic device with sufficient fidelity to create usable kinematic and dynamic models. This task was completed using a series of direct-measurement techniques, with a computer model generated using the defined parameters. It was found that this characterisation was accurate, with the exception of errors introduced by frictional effects. A comparison of commanding force values given by the same PD control algorithm running in simulation and on the actual device showed close correspondence, typically within 5%, confirming the validity of a model with sufficient fidelity for use in controller design.

The task of evaluating the Falcon's suitability as an entry-level delta-type robot for investigating and developing model based control and estimation methods for parallel robots is somewhat subjective. The authors believe that the platform is sufficient for this task, although admit that its suitability may be application dependant.

For the Falcon device to be useful as a robotic arm research platform, its functional specifications must be sufficiently representative of a more industrial robot platform for algorithm development. In particular, the system dynamics, actuation and measurement interfaces must be sufficient to allow the development of robust control and estimation algorithms which would avoid scaling issues when migrated to other platforms. The authors do not currently have access to other platforms to evaluate such migrations, however the simple PD controller used in the experiments of Section 6 show that the Falcon's actuation interface is sufficient to allow for high fidelity control in the face of significant system dynamics.

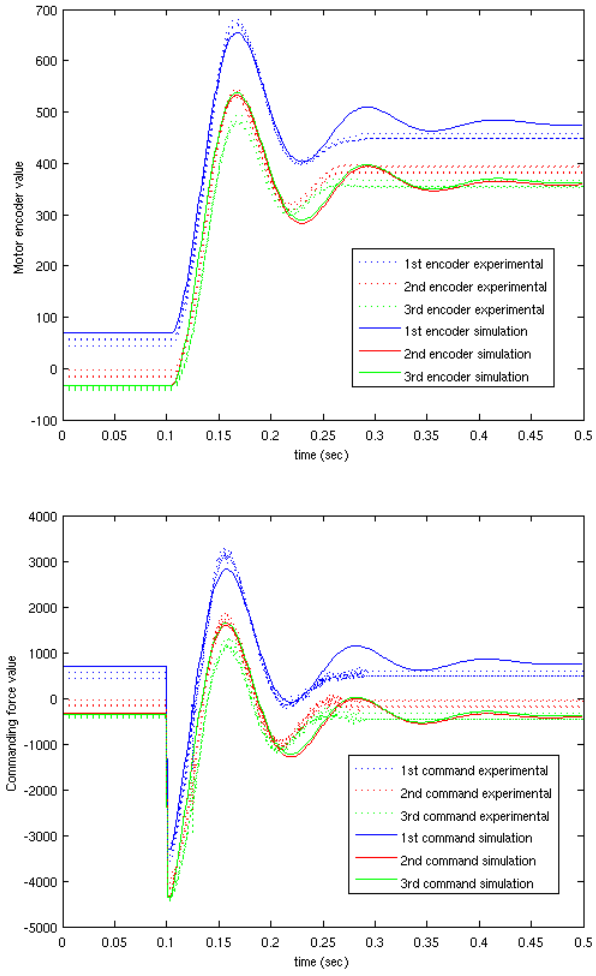

Figure 9: Comparison of executed trajectories (top) and commanding force values (bottom) for a point-to-point trajectory executed both on the Falcon itself, and in simulation. Data from four experimental runs are overlayed.

The authors consider the workspace volume and workspace resolution to be sufficient for control, planning and estimation algorithm development, however, the presented analysis has neglected any formal evaluation of backlash and joint slop which is likely to be the most significant factor retarding the Falcon's use as a research platform. The arm in it's intended orientation acts perpendicular to gravity, providing an effective pre-loading on joints when motion is low, but there is observable free-play at the end-effector during high-acceleration manoeuvres. The spring tensioning the actuation cable appears sufficient to remove any backlash in the actuation of the legs, and indeed is likely to be preferable to a geared system. The authors have developed a pen-holder to replace the standard end-effector which may be used for future formal evaluation of joint slop characteristics, but at this stage estimate the cumulative slop at the end-effector to be less than 1mm in any direction.

Simple calculations show that during the experiments of Section 6, the actuating legs underwent acceleration of the order of 1×10^3 degrees/s^2, with the encoder traces showing no step changes that would indicate evidence of significant system slop. Such trajectories also result in noticeable (but small) motion of the base on the desktop, suggesting that the device is capable of sufficient actuation force that the base should be rigidly fixed.

The most attractive feature of the Falcon for research purposes besides its form and availability, is the transparency of the control interface. We have direct access to a variable that we have shown can be easily translated to motor forces. This is as opposed to many commercial (non-research) robotic platforms whereby the internal firmware provides manufacturer developed control loops with only a velocity or position demand interface available to the user.

References

[Clavel, 1989] R. Clavel. Device for the movement and positioning of an element in space. United States Patent, 1989. Patent Number: 4976582.

[Corke and Armstrong-H'elouvry, 1994] P. Corke and B. Armstrong-H'elouvry. A search for consensus among model parameters reported for the puma 560 robot. In *IEEE Int. Conf. Robotics and Automation, Proceedings of*, pages 1608–1613, 1994.

[Grotjahn *et al.*, 2004] M. Grotjahn, B. Heimann, and A. Houssem. Identification of friction and rigid-body dynamics of parallel kinematic structures for model-based control. *Multibody System Dynamics*, 11, 2004.

[Huang *et al.*, 2007] T. Huang, P.F. Wang, J.P. Mei, X.M. Zhao, and D.G. Chetwynd. Time minimum trajectory planning of a 2-dof translational parallel robot for pick-and-place operation. *Annals of the CIRP*, 56(1), May 2007.

[Machulis, 2009] K. Machulis. libnifalcon: Open source driver for the Novint Falcon. http://libnifalcon.nonpolynomial.com, 2009.

[Miller, 2001] K. Miller. Dynamics of the nuew UWA robot. In *Australasian Conference on Robotics and Automation, Proceedings of*, Sydney, Australia, November 14-15 2001. Australian Robotics and Automation Association.

[Olsson, 2009] Andre. Olsson. Modelling and control of a delta-3 robot. Master's thesis, Lund University, February 2009.

[Ouellet, 2008] Kevin Ouellet. Projet de fin d'etudes en genie de la production automatisee. Technical report, University of Quebec, 2008.

[Palsbo *et al.*, 2008] S. E. Palsbo, D. Marr, W. Norbald, M. Hopkins, B. Bay, T. Streng, and B. Valenti. Desktop haptics for fine-motor hand rehabilitation (handwriting). In *Available at http://www.obslap.com*, December 2008.

[Pietsch *et al.*, 2003] I.T. Pietsch, O. Becker, M. Krefft, and J. Hesselbach. Time-optimal trajectory planning for adaptive control of plane parallel robots. In *Proceedings of the Fourth International Conference on Control and Automation*, Montreal, Canada, June 2003.

[Pietsch *et al.*, 2005] I.T. Pietsch, M. Krefft, O. Becker, C. Bier, and J. Hesselbach. How to reach the dynamic limits of parallel robots? an autonomous control approach. *IEEE Transactions on Automation Science and Engineering*, 2(4), October 2005.

[Schill *et al.*, 2008] F. Schill, R. Mahony, P. Corke, and L. Cole. Virtual force feedback teleoperation of the insectbot using optic flow. In *Australasian Conference on Robotics and Automation, Proceedings of*, Canberra, Australia, December 3-5 2008. Australian Robotics and Automation Association.

[Stamper, 1997] Richard E. Stamper. *A Three Degree of Freedom Parallel Manipulator with Only Translational Degrees of Freedom*. PhD thesis, University of Maryland, 1997.

[Streng, 2008] B. T. Streng. Mechanical linkage design for haptic rehabilitation and development of fine motor skills. Master's thesis, Oregon State University, December 2008.

[Tsai, 1997] Lung-Wen Tsai. Multi-degree-of-freedom mechanisms for machine tools and the like. United States Patent, 1997. Patent Number: 5,656,905.

[Wood and Kenedy, 2003] G.D. Wood and D.C. Kenedy. Simulating mechanical systems in Simulink with SimMechanics. Technical Report 91124v00, The MathWorks Inc., Natick, MA, 2003.